
DON'T USE LARGE MINI-BATCHES, USE LOCAL SGD

Tao Lin¹ Sebastian U. Stich¹ Martin Jaggi¹

ABSTRACT

Mini-batch stochastic gradient methods are the current state of the art for large-scale distributed training of neural networks and other machine learning models. However, they fail to adapt to a changing communication vs computation trade-off in a system, in particular when scaling to a large number of workers or devices. More so, the fixed requirement of communication bandwidth for gradient exchange in mini-batch SGD severely limits the scalability to multi-node training e.g. in datacenters, and even more so for training on decentralized networks such as mobile devices. We argue that variants of local SGD, which perform several update steps on a local model before communicating to other nodes, offer significantly improved overall performance and communication efficiency, as well as adaptivity to the underlying system resources. Furthermore, we present a new hierarchical extension of local SGD, and demonstrate that it can efficiently adapt to several levels of computation costs in a heterogeneous distributed system.

1 INTRODUCTION

The workhorse training algorithm for most machine learning applications—including deep-learning—is stochastic gradient descent (SGD). This algorithm is highly preferred over its classic counterpart, i.e. full gradient descent (GD), not only because it offers much cheaper iterations, but also because it can be more efficient in total number of gradient evaluations. This efficiency gain of SGD over GD is very well studied and known to reach up to a factor of n for sum-structured problems, both in theory (Shalev-Shwartz et al., 2010) and practice (Bottou, 2010), for n being the training set size. When considering overall computational cost, there seems no benefit in evaluating multiple stochastic gradients at the same time, such as done in mini-batch SGD. However, the latter algorithm can easily be parallelized among different workers, which makes it a better choice for modern distributed deep-learning applications for two reasons: (i) mini-batch SGD can exploit the compute parallelism locally available on modern computing devices such as GPUs. The second reason is that (ii) less frequent parameter updates do help alleviate the communication bottleneck between the worker devices, which is crucial in a distributed setting, in particular for large models.

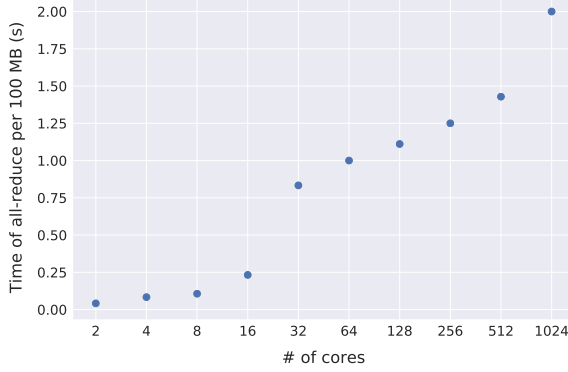
Recent applications (Goyal et al., 2017; You et al., 2017a) aim at reducing training time in the distributed setting by using many machines and running SGD with dramatically

larger mini-batch size than reported previously in the literature. However, we claim that this choice of large batches is often taken for the wrong reason—namely just to saturate computation—while not correctly trading-off the efficiency benefits of sequential SGD (which can be run locally on each worker) over full GD (as the limit of very large batches). Additionally, when scaling up the number of worker devices, the parallelism per device remains unchanged as a limiting factor, while the communication efficiency often decreases dramatically (see e.g. Figure 1(a)).

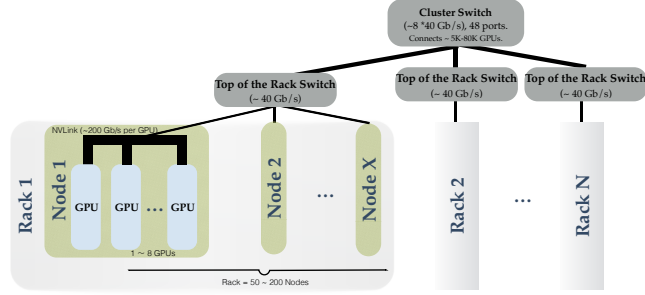
To solve this issue, and at the same time still allow adaptivity to the computation/communication trade-off, we propose to use novel variants of local SGD (McDonald et al., 2009; Zinkevich et al., 2010a; Zhang et al., 2016) on each worker. Local SGD schemes update the parameters by averaging between the workers only after several local steps (without communication). We demonstrate that tuning the number of local steps between the communication rounds successfully decouples the two aspects of local parallelism and communication latency. Furthermore, the resulting training scheme leads to a significant decrease of the overall training time as well as improved scalability and robustness as the number of workers increases.

Furthermore, we leverage this idea to the more general setting of training on decentralized and heterogeneous systems, which is an increasingly important application area. Such systems have become common in industry, e.g. with GPUs or other accelerators grouped hierarchically within machines, racks or even at the level of several data-centers. Hierarchical system architectures such as in Figure 1(b) motivate our hierarchical extension of local SGD. Moreover,

¹School of computer and communication science, EPFL, Lausanne, Switzerland. Correspondence to: Tao Lin <tao.lin@epfl.ch>.



(a) The data transmission cost (in seconds) of an all-reduce operation for 100 MB, over the different number of cores, using PyTorch's built-in MPI all-reduce operation. Each evaluation is the average result of 100 data transmissions on a Kubernetes cluster. The network bandwidth is 10 Gbps, and we use 48 cores per physical machine.



(b) Illustration of a hierarchical network architecture of a cluster in the data center. While GPUs within each node are linked with fast connections (e.g. NVLink), connections between the servers within and between different racks have much lower bandwidth and latency (via top-of-the-rack switches and cluster switches). The hierarchy can be extended several layers further and further. Finally, edge switches face the external network at even lower bandwidth.

Figure 1. The motivation for (hierarchical) local SGD from a systems perspective.

end-user devices such as mobile phones form huge heterogeneous networks, where the benefits of efficient distributed and data-local training of machine learning models promises strong benefits in terms of data privacy.

Our main contributions can be summarized as follows:

- We demonstrate that local SGD training schemes can achieve state-of-the-art accuracy at significantly reduced training time as well as reduced communication cost, for a variety of deep learning models including computer vision tasks, when training on distributed commodity hardware systems. While the algorithm itself is not novel, this systematic study to our knowledge is the first in showing consistent improvements compared to SGD baselines including recent large-batch methods (Goyal et al., 2017). In particular, we also show that a significant speedup remains robust when scaling the number of workers K , and that generalization accuracy degrades much more gracefully with large K compared to existing large-batch training methods.
- We propose a novel hierarchical extension of the local SGD training framework, further improving the adaptivity of local SGD to a wide range of real-world heterogeneous distributed systems. We show that in a realistic setting of training over multiple servers or datacenters, hierarchical local SGD offers significantly better performance compared to both local SGD and mini-batch SGD, in terms of communication efficiency, to reach the same accuracy.

2 RELATED WORK

While mini-batch and parallel SGD are very well studied (Takáč et al., 2013; Zinkevich et al., 2010b), the theoretical understanding of local SGD variants is less clear. A parallel version of local SGD has been empirically studied in (Zhang et al., 2016). For a sub-class of convex models, Biral et al. (2016) studies local SGD in the setting of a general graph of workers. The theoretical convergence analysis has remained elusive for a long time, see e.g. (Alistarh et al., 2018), until the very recent work of Stich (2018) which addresses the convergence rate in the convex case, and both Zhou & Cong (2018) and (Yu et al., 2018) address the non-convex case. Here we focus on (synchronous) distributed SGD in large scale applications, under the plain map-reduce communication model. Our viewpoint is not specific to neural-network models, but applies to general sum structured distributed optimization objectives.

Asynchronous SGD algorithms (Chilimbi et al., 2014; Dean et al., 2012) aim to improve overall training time at the expense of additional noise introduced from asynchrony, i.e. updates coming from gradients computed at stale weight vectors. Chen et al. (2016) demonstrates that synchronous distributed SGD offers improved performance for deep learning workloads and is able to alleviate the staleness impact of asynchronous SGD. Current state-of-the-art distributed deep learning frameworks (Abadi et al., 2016; Paszke et al., 2017; Seide & Agarwal, 2016) resort to synchronized large-batch training, allowing scaling by adding more computational units and performing data-parallel synchronous SGD with mini-batches divided between devices. In order to improve the overall efficiency of mini-batch

SGD training, those methods are restricted to increasing the batch size, while keeping the workload constant on each device. It has been shown that training with large batch size (e.g. batch size $> 10^3$ for the case of ImageNet) typically degrades the performance both in terms of training and test error (Goyal et al., 2017; Chen & Huo, 2016; Hoffer et al., 2017; Keskar et al., 2016; Li, 2017; Li et al., 2014). Goyal et al. (2017) suggests performing a “learning rate warm-up” phase with linear scaling of the step-size, successfully training ImageNet with a ResNet-50 network with batch size 8K (to the level of 76.26% accuracy).

For training in a massively distributed scenario, the work of (Konecny et al., 2015; 2016; McMahan et al., 2017) introduces the setting of federated learning. While other stochastic approaches such as e.g. (Zhang et al., 2015; Wang et al., 2017), require iid distributed data, this is not required in the federated setting. However, none of these algorithms address the task of training on a multi-level heterogeneous system. Another promising line of research addressing the communication bottleneck of large scale training is to use quantization (Alistarh et al., 2017; Zhou et al., 2016; Wen et al., 2017) or more aggressive sparsification (Aji & Heafield, 2017; Lin et al., 2017; Strom, 2015) of gradients. These techniques are orthogonal to our scheme and can offer promising savings when applied at the level of communication between the nodes.

3 LOCAL SGD

We consider standard sum-structured optimization problems of the form $\min_{\mathbf{w} \in \mathbb{R}^d} \frac{1}{n} \sum_{i=1}^n f_i(\mathbf{w})$, where \mathbf{w} are the parameters of the model (e.g. neural network), and f_i is the loss function of the i -th training data example.

The mini-batch update of SGD is given by

$$\mathbf{w}_{t+1} := \mathbf{w}_t - \gamma_t \left[\frac{1}{|\mathcal{I}_t|} \sum_{i \in \mathcal{I}_t} \nabla f_i(\mathbf{w}_t) \right], \quad (1)$$

where $\mathcal{I}_t \subseteq [n]$ is a subset of indices of the n training datapoints, typically selected uniformly at random, and γ_t denotes the step-size (concrete values will be given below). $B := |\mathcal{I}_t|$ denotes the batch size, and the three update schemes of SGD, mini-batch SGD and GD respectively can be represented by $|\mathcal{I}_t| = 1$, $|\mathcal{I}_t| = B$ and $|\mathcal{I}_t| = n$. In the distributed setup, data examples are partitioned across K devices (such as GPUs or cloud compute nodes), each only having access to its local training data. The workhorse algorithm in this setting is again mini-batch SGD,

$$\mathbf{w}_{t+1} := \mathbf{w}_t - \gamma_t \left[\frac{1}{K|\mathcal{I}_t^k|} \sum_{k=1}^K \sum_{i \in \mathcal{I}_t^k} \nabla f_i(\mathbf{w}_t) \right], \quad (2)$$

where now the mini-batch of the k -th device is formed from local data \mathcal{I}_t^k , and the K devices compute gradients in parallel and then synchronize the local gradients by averaging.

3.1 The Local SGD Algorithm

In contrast to mini-batch SGD, local SGD performs local sequential updates on each device, before aggregating the updates between the K devices, as illustrated in Figure 2.

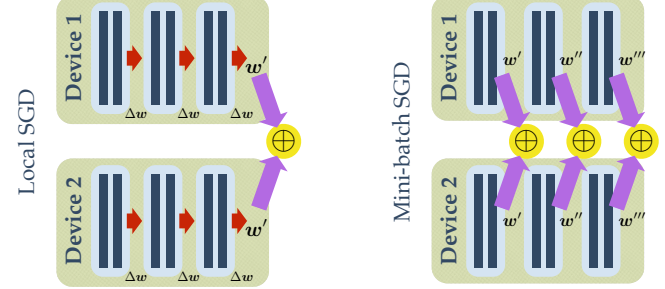


Figure 2. One round of local SGD (left) versus mini-batch SGD (right). In both settings $B_{\text{loc}} = 2$. For the local variant, we have $H = 3$ local steps. Local parameter updates are depicted in red, whereas global averaging (synchronization) is depicted in purple.

Each worker k iteratively samples small mini-batches of fixed size B_{loc} , from its local data \mathcal{I}^k . It then sequentially performs $H \geq 1$ local parameter updates, before performing global parameter aggregation with the other devices. Therefore, per synchronization/communication, local SGD accesses $B_{\text{glob}} = H \cdot B_{\text{loc}}$ training examples (gradient computations) on each device.

Formally, one round of local SGD can be described as

$$\mathbf{w}_{(t)+H}^k := \mathbf{w}_{(t)}^k - \sum_{h=1}^H \frac{\gamma_{(t)}}{B_{\text{loc}}} \cdot \sum_{i \in \mathcal{I}_{(t)+h-1}^k} \nabla f_i(\mathbf{w}_{(t)+h-1}^k), \quad (3)$$

where $\mathbf{w}_{(t)+h}^k$ denotes the local model on machine k after t global synchronization rounds and subsequent h local steps. The definition of $\gamma_{(t)}$ and $\mathcal{I}_{(t)+h-1}^k$ follows the same scheme.

After H local updates the synchronized global model $\mathbf{w}_{(t+1)}^k$ is obtained by averaging $\mathbf{w}_{(t)+H}^k$ among the K workers as in an all-reduce communication pattern

$$\mathbf{w}_{(t+1)}^k := \mathbf{w}_{(t)}^k - \frac{1}{K} \sum_{k=1}^K (\mathbf{w}_{(t)}^k - \mathbf{w}_{(t)+H}^k). \quad (4)$$

Later, we will modify the update scheme of local SGD in (4) to include momentum, see Appendix D.1.1 for details.

3.2 Hierarchical Local SGD

Real world systems come with different communication bandwidths on several levels. In this scenario, we propose to employ local SGD on each level of the hierarchy, adapted to each corresponding computation vs communication trade-off. The resulting scheme, hierarchical local SGD, offers

significant benefits in system adaptivity and performance as we will see in the rest of the paper.

As the guiding example, we consider compute clusters which typically allocate a large number of GPUs grouped over several machines, and refer to each group as a GPU-block. Hierarchical local SGD continuously updates the local models on each GPU for a number of H *local update steps* before a (fast) synchronization within a GPU-block. On the outer level, after H^b such *block update steps*, a (slower) global synchronization over all GPU-blocks is performed. Figure 3 and Algorithm 2 (refer to the appendix) depict how the hierarchical local SGD works, and the complete procedure is formalized below:

$$\begin{aligned} \mathbf{w}_{[(t)+l]+H}^k &:= \mathbf{w}_{[(t)+l]}^k - \sum_{h=1}^H \frac{\gamma_{[(t)]}}{B_{\text{loc}}} \cdot \sum_{i \in \mathcal{I}_{[(t)+l]+h-1}^k} \nabla f_i(\mathbf{w}_{[(t)+l]+h-1}^k) \\ \mathbf{w}_{[(t)+l+1]}^k &:= \mathbf{w}_{[(t)+l]}^k - \frac{1}{K_i} \sum_{k=1}^{K_i} (\mathbf{w}_{[(t)+l]}^k - \mathbf{w}_{[(t)+l]+H}^k) \\ \mathbf{w}_{[(t+1)]}^k &:= \mathbf{w}_{[(t)]}^k - \frac{1}{K} \sum_{k=1}^K (\mathbf{w}_{[(t)]}^k - \mathbf{w}_{[(t)+H^b]}^k) \end{aligned} \quad (5)$$

where $\mathbf{w}_{[(t)+l]+H}^k$ indicates the model after l block update steps and H local update steps, and K_i is the number of GPUs on the GPU-block i . The definition of $\gamma_{[(t)]}$ and $\mathcal{I}_{[(t)+l]+h-1}^k$ follows a similar scheme.

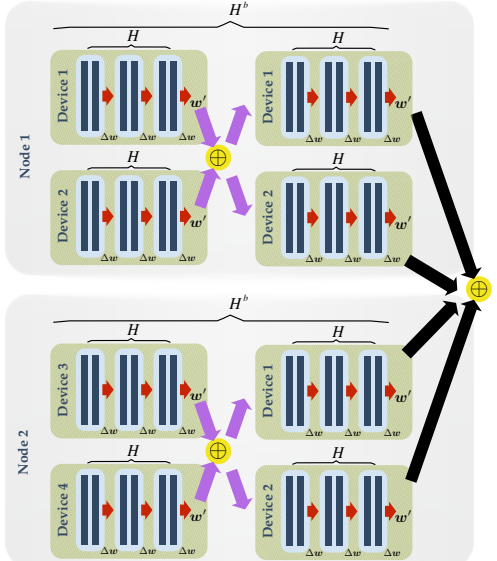


Figure 3. An illustration of hierarchical local SGD, for $B_{\text{loc}} = 2$, using $H = 3$ local steps and $H^b = 2$ block steps. Local parameter updates are depicted in red, whereas block and global synchronization is depicted in purple and black respectively.

As the number of devices grows to the thousands (Goyal et al., 2017; You et al., 2017a), the difference between ‘within’ and ‘between’ block communication efficiency becomes more drastic. Thus, the performance benefits of our

adaptive scheme compared to flat & large mini-batch SGD will be even more pronounced.

3.3 Convergence Theory of Local SGD

The main advantage of local SGD over mini-batch SGD is the drastic reduction in the amount of communication, when accessing the same number of datapoints or gradients. However, this advantage would be in vain if the convergence of local SGD would be slower than the one of mini-batch SGD. In this following section we therefore consider the theoretical convergence properties for local SGD.

First we discuss the convex setting. It is well-known that an individual run of SGD on a single machine converges as $\mathcal{O}((THB_{\text{loc}})^{-1})$, see e.g. (Lacoste-Julien et al., 2012). By convexity, we can derive that averaging K instances of such local SGD executions will only improve the attained training objective value. However, this simple argument is not enough to quantify the speed-up of local SGD, i.e. does not allow to incorporate K in the rate. This is still an active area of research (cf. also (Alistarh et al., 2018; Stich, 2018)). Stich (2018) very recently showed linear speed-up, i.e. convergence at rate $\mathcal{O}((KTHB_{\text{loc}})^{-1})$ for strongly convex and smooth objective functions.

Two recent theoretical contributions shed some light on local SGD in the non-convex setting. For smooth objective functions, Zhou & Cong (2018) show a rate $\mathcal{O}((KTB_{\text{loc}})^{-1/2})$ which only coincides in the extreme case $H = 1$ with the rate of mini-batch SGD. Yu et al. (2018) give an improved result $\mathcal{O}((HKTB_{\text{loc}})^{-1/2})$.

All those results assume a fixed communication frequency H . However, it is not clear yet whether this is the best choice in general. Intuitively, one would expect when the diversity of the local sequences $\mathbf{w}_{(t)+h}^k$ is small, for instance measured as $\frac{1}{K} \sum_{k=1}^K \mathbb{E} \|\bar{\mathbf{w}}_{(t)+h}^k - \mathbf{w}_{(t)+h}^k\|^2$ for $\bar{\mathbf{w}}_{(t)+h}^k := \frac{1}{K} \sum_{k=1}^K \mathbf{w}_{(t)+h}^k$; then one has to communicate less frequently. On the other hand when the difference between the sequences is larger (such as expected at the beginning of the training process) then one should communicate updates more frequently. Zhang et al. (2016) empirically studied the effect of the averaging frequency on the quality of the solution for some problem cases. They observe that more frequent averaging at the beginning of the optimization can help and bring forward a theoretical illustration that supports this finding. Also Bijral et al. (2016) argue to average more frequently at the beginning. Thus, we will adopt such a strategy later in the experiments.

3.4 Numerical Illustration on a Convex Problem

Before moving to our deep learning experiments, we first illustrate the convergence properties of local SGD on a

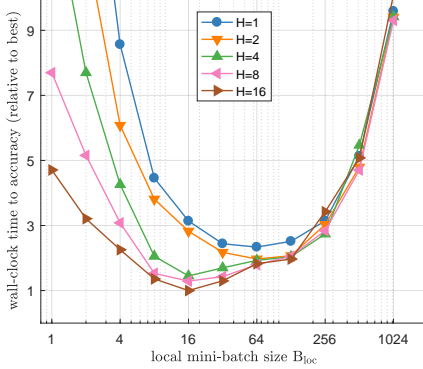


Figure 4. Time (relative to best method) to solve a regularized logistic regression problem to target accuracy $\epsilon = 0.005$ for $K = 16$ workers for $H \in \{1, 2, 4, 8, 16\}$ and local mini-batch size B_{loc} . We simulate the network traffic under the assumption that communication is $25 \times$ slower than a stochastic gradient computation.

small scale convex problem. For this, we consider logistic regression on the w8a dataset¹ ($d = 300, n = 49749$). We measure the number of iterations to reach the target accuracy $\epsilon = 0.005$. For each combination of H, B_{loc} and K we determine the best learning rate by extensive grid search (cf. Section E for the detailed experimental setup). In order to mitigate extraneous effects on the measured results, we here measure time in discrete units, that is we count the number of stochastic gradient computations and communication rounds, and assume that communication of the weights is $25 \times$ more expensive than a gradient computation, for ease of illustration.

Figure 4 shows that different combinations of the parameters (B_{loc}, H) can impact the convergence time for $K = 16$. Here, local SGD with $(16, 16)$ converges more than $2 \times$ faster than for $(64, 1)$ and $3 \times$ faster than for $(256, 1)$.

Figure 5 depicts the speedup when increasing the number of workers K . Local SGD shows the best speedup for $H = 16$ on a small number of workers, while the advantage gradually diminishes for very large K .

4 LOCAL SGD FOR DEEP LEARNING

4.1 Experimental Setup

In this section, we empirically compare mini-batch SGD and the proposed (hierarchical) local SGD. First we describe the experimental setup.

Datasets. We use the following classification tasks.

- CIFAR-10/100 (Krizhevsky & Hinton, 2009). Each consist of a training set of 50K and a test set of 10K

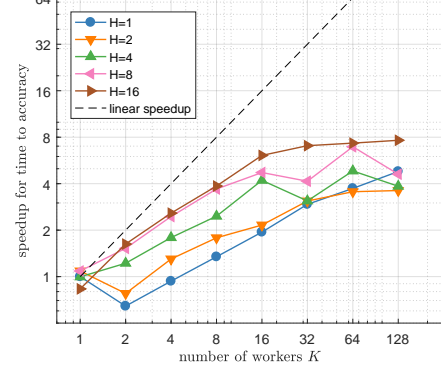


Figure 5. Speedup over the number of workers K to solve a regularized logistic regression problem to target accuracy $\epsilon = 0.005$, for $B_{\text{loc}} = 16$ and $H \in \{1, 2, 4, 8, 16\}$. We simulate the network traffic under the assumption that communication is $25 \times$ slower than a stochastic gradient computation.

color images of 32×32 pixels, as well as 10 and 100 target classes respectively. We adopt the standard data augmentation scheme and preprocessing scheme (He et al., 2016a; Huang et al., 2016b).

- ImageNet (Russakovsky et al., 2015). The ILSVRC 2012 classification dataset consists of 1.28 million images for training, and 50K for validation, with 1K target classes. We use ImageNet-1k (Deng et al., 2009) and adopt the same data preprocessing and augmentation scheme as in (He et al., 2016a;b; Simonyan & Zisserman, 2014). The network input image is a 224×224 pixel random crop from augmented images, with per-pixel mean subtracted.

Models. We use ResNet-20 (He et al., 2016a) on CIFAR-10/100 to investigate the performance of (hierarchical) local SGD, and then use ResNet-50 on the challenging ImageNet to investigate the accuracy and scalability of (hierarchical) local SGD. We also run experiments on DenseNet (Huang et al., 2016a) and WideResNet (Zagoruyko & Komodakis, 2016) to demonstrate the generalization ability of local SGD for different models.

Model initialization. We here only mention some shared strategies for model initialization. Model-specific initialization schemes, e.g., the use of momentum scheme, can be found in the experimental sections below. For all models, we use a weight decay λ of $1e-4$ and, following He et al. (2016a), we do not apply weight decay on the learnable Batch Normalization (BN) coefficients. For the weight initialization we follow Goyal et al. (2017) where we adopt the initialization introduced by He et al. (2015) for convolution layers, and initialize fully-connected layer from a zero-mean Gaussian distribution with the standard deviation of 0.01.

¹www.csie.ntu.edu.tw/~cjlin/libsvmtools/datasets/binary.html

For the BN for distributed training we again follow Goyal et al. (2017) and compute the BN statistics independently for each worker.

Implementation and platform. We implement² (hierarchical) local SGD in PyTorch (Paszke et al., 2017), with a flexible configuration of the machine topology supported by Kubernetes. The cluster consists of 15 $2 \times$ Intel Xeon E5-2680 v3 servers and has 30 NVIDIA TITAN Xp GPUs in total. In the rest of the paper, we use $a \times b$ -GPU to denote the topology of the cluster, i.e., a nodes and each with b GPUs.

Large-batch learning tricks We refer the tricks proposed recently for the efficient large batch training (Goyal et al., 2017), as “large-batch learning tricks”. The tricks are formalized by the following two configurations: (1) linearly scaling the learning rate w.r.t. the global mini-batch size; (2) gradually warmup the learning rate from a small value. See Appendix C for more details.

4.2 Local SGD Training

4.2.1 Training ResNet-20 on CIFAR-10/100

In our first experiments with local SGD, we train ResNet-20 for CIFAR-10 with varied number of GPUs from $K = 2$ to $K = 16$. We show that *local SGD is an easy plugin alternative for mini-batch SGD, with significantly improved communication efficiency and guaranteed performance*.

The experiments follow the common mini-batch SGD training scheme for CIFAR (He et al., 2016a;b) and all competing methods access the same total amount of data samples regardless of the number of local steps or block steps. More precisely, the training procedure is terminated when the distributed algorithms have accessed the same number of samples as a standalone worker would access in 300 epochs. The data is partitioned among the GPUs and reshuffled globally every epoch. The local mini-batches are then sampled among the local data available on each GPU. The learning rate scheme is the same as in (He et al., 2016a), where the initial learning rate starts from 0.1 and is divided by 10 when the model has accessed 50% and 75% of the total number of training samples. In addition to this, the momentum parameter is set to 0.9 without dampening, and applied independently to each local model.³

The training procedure mentioned above is kept consistent across the local SGD and hierarchical local SGD experiments, and unless stated otherwise, no specific treatments such as special learning rate schemes have been used.

² Our code will be made publicly available.

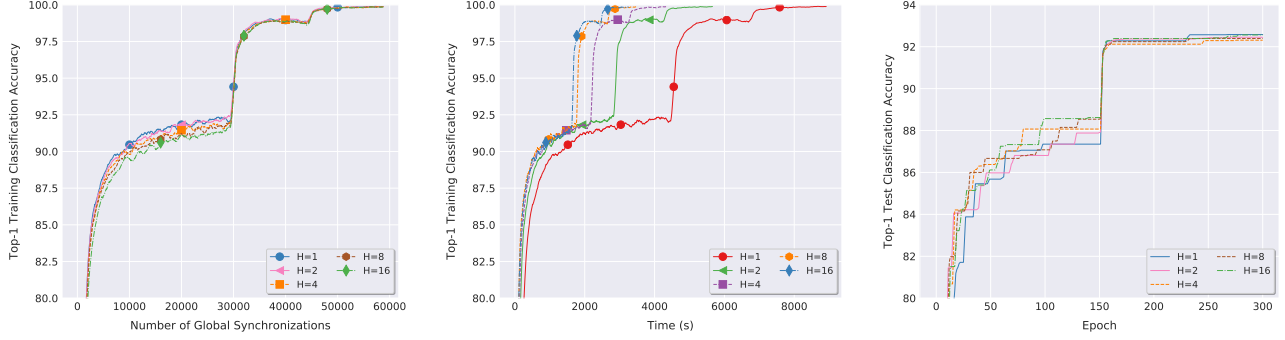
³ The investigation of local momentum and global momentum can be found in the supplementary material.

Better communication efficiency, with guaranteed test accuracy. Figure 6 shows that *local SGD is significantly more communication efficient while guaranteeing the same accuracy and enjoys faster convergence speed*. In Figure 6, the local models use a fixed local mini-batch size $B_{\text{loc}} = 128$ for all updates. All methods run for the same number of total gradient computations. Mini-batch SGD—the baseline method for comparison—is a special case of local SGD with $H = 1$, with full global model synchronization for each local update. We see that local SGD with $H > 1$, as illustrated in Figure 6(a), by design does H times less global model synchronizations, alleviating the communication bottleneck while accessing the same number of samples. The impact of local SGD training upon the total training time is more significant for larger number of local steps H (i.e., Figure 6(b)), resulting in an at least $3 \times$ speed-up when comparing mini-batch $H = 1$ to local SGD with $H = 16$. The reached final training accuracy remains stable across different H values, and there is no difference or negligible difference in test accuracy (Figure 6(c)). The analogue experiments for the CIFAR-100 datasets are provided in the supplementary material, as well as the performance of local SGD on DenseNet and WideResNet in Table 5.

Better generalization performance than “large batch training”. Table 1 demonstrates that *local SGD offers better generalization performance than mini-batch SGD, when accessing the same number of samples (gradient computations) per device per global synchronization*. Goyal et al. (2017) propose large-batch learning tricks to improve the poor generalization of large-batch training methods. Table 1 shows the top-1 test accuracy of a ResNet-20 trained for CIFAR-10 with varied numbers of gradient computations B_{glob} , keeping either B_{loc} fixed to 128 (local SGD), or keeping $H = 1$ (large-batch SGD). In this experiment, the large-batch learning tricks do not solve the problem for large B_{glob} , while local SGD enjoys stable generalization.

Significantly better scalability when increasing the number of workers. Figure 7(a) demonstrates the speedup in time-to-accuracy for training ResNet-20 for CIFAR-10, with varying number of GPUs K from 2 to 16 and local update steps H from 1 to 16. $H = 1$ corresponds to the mini-batch SGD case. The communication is on top of an 8×2 -GPU cluster with 10 Gbps network bandwidth. The speedup in Figure 7(a) measures the inverse ratio of the training time on any number of GPUs versus the time on 1×2 -GPU, to reach the top-1 test accuracy of CIFAR-10 of 91.2% (which was the accuracy reached by all competitors). The test accuracy is evaluated each time when the distributed algorithm has accessed the complete training dataset.

We demonstrate in Figure 7(a) that *local SGD scales 2× better than its mini-batch SGD counterpart, in terms of time*.



(a) Training accuracy vs. number of global synchronization rounds.

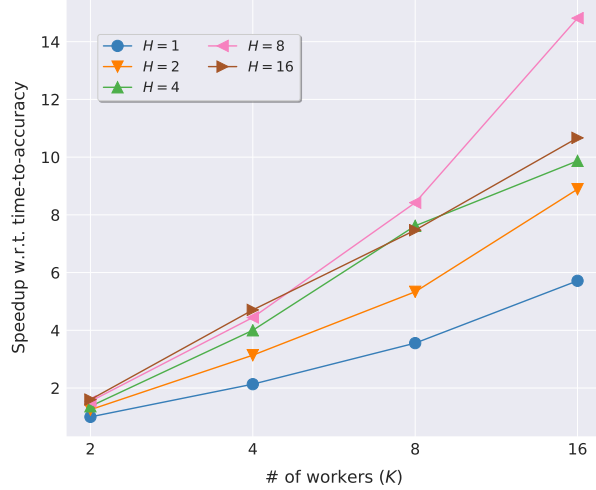
(b) Training accuracy vs. training time.

(c) Test accuracy vs. number of epochs.

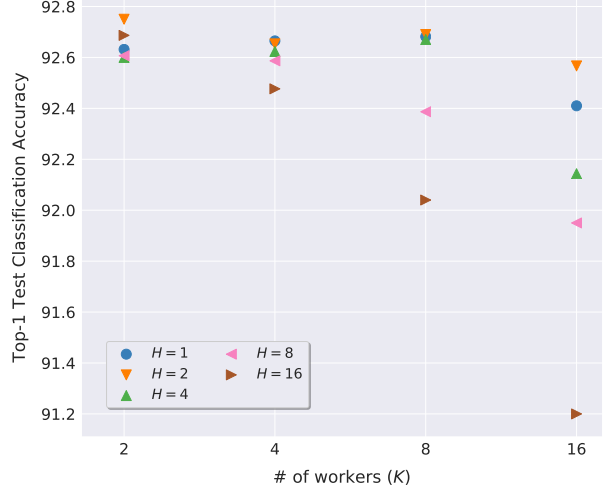
Figure 6. Training **CIFAR-10** with **ResNet-20** via **local SGD** (2×1 -GPU). The local batch size B_{loc} is fixed to 128, and the number of local steps H is varied from 1 to 16. The experiments are using the same hyper-parameters, except the local update steps H .

Table 1. Training **CIFAR-10** with **ResNet-20** via **local SGD** (2×1 -GPU). The top-1 **test accuracy** of mini-batch SGD and local SGD is reported, for a fixed number of accessed samples per synchronization B_{glob} . Note that local SGD will always fix the batch size $B_{\text{loc}} = 128$ but vary the number of local update steps H , while mini-batch SGD always keeps $H = 1$ and $B_{\text{loc}} = B_{\text{glob}}$. The reported results are the average of three runs. 'w/ tricks' refers to the large-batch learning tricks (Goyal et al., 2017) (cf. supplementary material), which we also compare to the corresponding default configurations for completeness and fair comparison.

		$B_{\text{glob}} = 128$	$B_{\text{glob}} = 256$	$B_{\text{glob}} = 512$	$B_{\text{glob}} = 1024$	$B_{\text{glob}} = 2048$	$B_{\text{glob}} = 4096$
w/o tricks	Local SGD	91.84 ± 00.10	92.06 ± 00.16	92.42 ± 00.08	92.08 ± 00.07	92.13 ± 00.12	92.00 ± 00.06
	Mini-batch	91.84 ± 00.10	91.96 ± 00.13	91.47 ± 00.28	90.42 ± 00.54	88.96 ± 01.36	59.17 ± 23.64
w/ tricks	Local SGD	92.63 ± 00.07	92.75 ± 00.09	92.60 ± 00.03	92.61 ± 00.14	92.69 ± 00.19	92.30 ± 00.10
	Mini-batch	92.63 ± 00.07	92.38 ± 00.09	92.55 ± 00.10	92.21 ± 00.07	43.79 ± 25.80	13.90 ± 03.91



(a) **Speedup** over single node (1×2 -GPU) training time for reaching 91.2% top-1 test accuracy under different K and H .



(b) Top-1 **test accuracy** of training under different K and H . All settings access to the same total number of training samples.

Figure 7. Scaling behavior of **local SGD** for increasing number of workers K , for different number of local update steps H , for training **ResNet-20** on **CIFAR-10**. Note that $H = 1$ is mini-batch SGD. The local batch size is fixed to $B_{\text{loc}} = 128$. We use a 8×2 -GPU cluster with 10 Gbps network bandwidth. Results are averaged over three runs.

to-accuracy under increasing the number of workers K . The benefits brought by local update steps H further show their advantages over the current large-batch training, where the current common “large-batch” SGD fixes the local mini-batch size B_{loc} and increases the number of workers K . The parallelism per device remains unchanged while facing the communication overhead. In this experiment, local SGD on 8 GPUs with $H = 8$ even achieves a $2 \times$ lower time-to-accuracy than mini-batch SGD with 16 GPUs. Moreover, the (near) linear scaling performance for $H = 8$ in Figure 7(a), shows that the main hyper-parameter H of local SGD is robust and consistently away from its mini-batch counterpart, under scaling the number of workers.

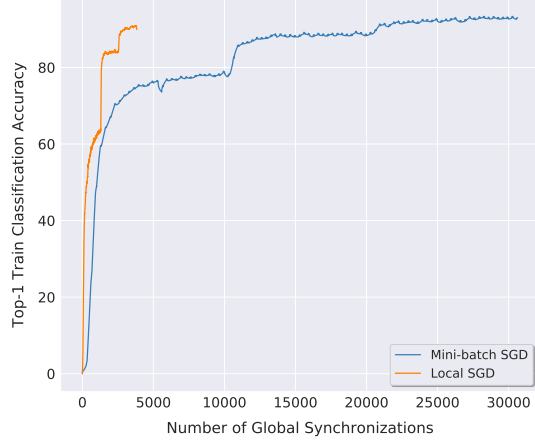
In summary, *Local SGD improves system scalability and reliability in practice*. Figure 7(b) shows that this comes without sacrificing generalization performance in terms of test accuracy. Local SGD easily reaches the state-of-the-art results of ResNet-20 on CIFAR-10, and achieves similar or better top-1 test accuracy compared to its mini-batch SGD counterpart.

4.2.2 Training ResNet-50 on ImageNet-1k

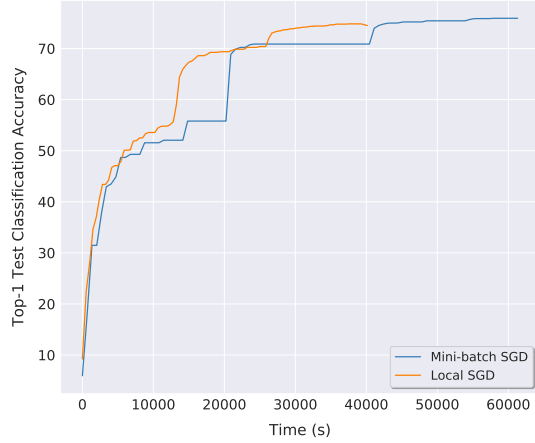
While in Section 4.2.1 above we have explored and better understood the performance of local SGD on the CIFAR-10 dataset, this section demonstrates the successfully scaling of local SGD to large datasets and larger clusters. Local SGD presents to be a competitive alternative to the current large-batch ImageNet training methods. Figure 8(a) and Figure 8(b) below show that we can efficiently (at least $1.5 \times$) train state-of-the-art ResNet-50 (He et al., 2016a; Goyal et al., 2017; You et al., 2017b) for ImageNet via local SGD on a 15×2 -GPU Kubernetes cluster.

We limit ResNet-50 training to 90 passes over the data in total, and the data is disjointly partitioned and is re-shuffled globally every epoch. We adopt the large-batch learning tricks (Goyal et al., 2017) below. We linearly scale the learning rate based on # of GPUs $\times \frac{0.1}{256}$ where 0.1 and 256 is the base learning rate and mini-batch size respectively for standard single GPU training. The local mini-batch size is set to 128. For learning rate scaling, we perform gradual warmup for the first 5 epochs, and decay the scaled learning rate by the factor of 10 when local models have access 30, 60, 80 epochs of training samples respectively. Moreover, in our ImageNet experiment, the initial phase of local SGD training follows the theoretical assumption mentioned in Subsection 3.3, and thus we gradually warm up the number of local steps from 1 to the desired value H during the first few epochs of the training⁴.

⁴ In our local SGD experiment for ImageNet, we found that exponentially increasing the number of local steps from 1 by the factor of 2 (until reaching the expected local step number) performs well. For example, our ImageNet training uses $H = 8$, so the



(a) Training top-1 classification accuracy of local SGD and mini-batch SGD w.r.t. the number of global synchronizations.



(b) Test top-1 accuracy of local SGD and mini-batch SGD in terms of time.

Figure 8. The performance of **local SGD** trained on **ImageNet-1k** with **ResNet-50** on a 15×2 -GPU cluster. We evaluate the model performance on test dataset after each complete accessing of the whole training samples. We apply the large-batch learning tricks (Goyal et al., 2017) to the ImageNet for these two methods. For local SGD, the number of local steps is set to $H = 8$.

4.3 Hierarchical Local SGD Training

Now we move to our proposed training scheme for distributed heterogeneous systems. In our experimental setup we try to mimic the real world setting where several compute devices such as GPUs are grouped over different servers, and where network bandwidth (e.g. Ethernet) limits the communication of updates of large models. The investigation of hierarchical local SGD again trains ResNet-20 on CIFAR-10 and follows the same training procedure as local SGD.

number of local update steps for the first three epochs are 1, 2, 4 respectively.

Table 2. Training CIFAR-10 with ResNet-20 via local SGD on a 8×2 -GPU cluster. The local batch size B_{loc} is fixed to 128 with $H^b = 1$, and we scale the number of local step H from 1 to 1024. The reported **training times** are the average of three runs and all the experiments are under the same training configurations for the equivalent of 300 epochs, without specific tuning.

$H =$	1	2	4	8	16	32	64	128	256	512	1024
Training Time (minutes)	20.07	13.95	10.48	9.20	8.57	8.32	9.22	9.23	9.50	10.30	10.65

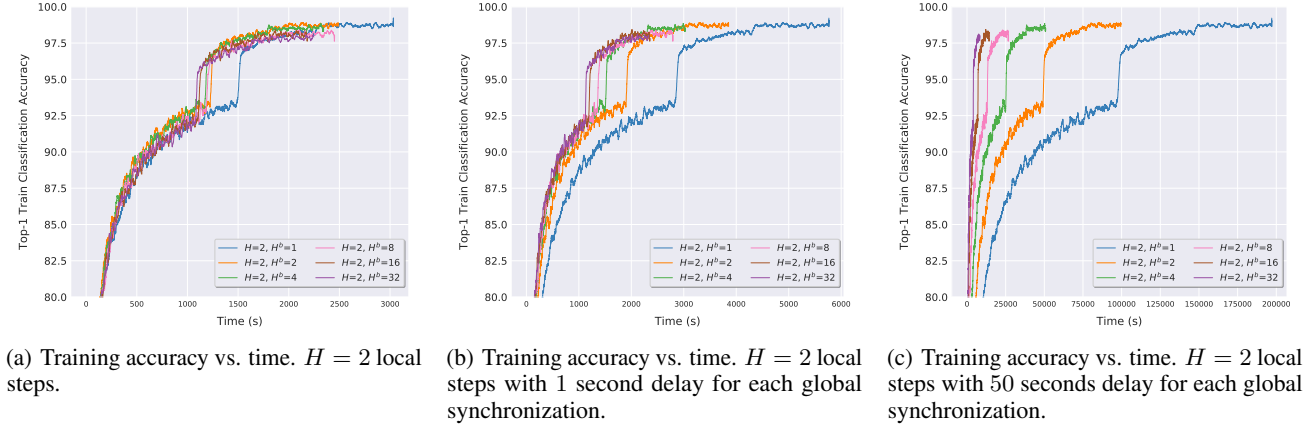


Figure 9. The performance of **hierarchical local SGD** trained on **CIFAR-10** with **ResNet-20** (2×2 -GPU). Each GPU block of the hierarchical local SGD has 2 GPUs, and we have 2 blocks in total. Each figure fixes the number of local steps but varies the number of block steps from 1 to 32. All the experiments are under the same training configurations, without specific tuning.

Training time vs. local number of steps. Table 2 shows the performance of local SGD in terms of training time. The communication traffic comes from the global synchronization over 8 nodes, each having 2 GPUs. We can witness that increasing the number of local update steps over the “datacenter” scenario cannot infinitely improve the communication performance, or would even reduce the communication benefits brought by large number of local updates. *Hierarchical local SGD with inner node synchronization reduces the difficulty of synchronizing over the complex heterogeneous environment, and hence enhances the overall system performance of the synchronization. The benefits are further pronounced when scaling up the cluster size.*

Hierarchical local SGD shows high tolerance to network delays. Even in our small-scale experiment of two servers and each with two GPUs, *hierarchical local SGD shows its ability to significantly reduce the communication cost by increasing the number of block step H^b (for a fixed H), with trivial performance degradation. Moreover, hierarchical local SGD with a sufficient number of block steps offers strong robustness to network delays.* For example, for fixed $H = 2$, by increasing the number of H^b , i.e. reducing the number of global synchronizations over all models, we obtain a significant gain in training time as in Figure 9(a). The impact of a network of slower communication is further studied in Figure 9(b), where the training is simulated in

a realistic scenario and each global communication round comes with an additional delay of 1 second. Surprisingly, even for the global synchronization with straggling workers and has occurred a much more severe 50 seconds delay per global communication round, Figure 9(c) demonstrates that a large number of block steps (e.g. $H^b = 16$) still manages to fully overcome the communication bottleneck with no/trivial performance damage.

Hierarchical local SGD offers improved scaling and better test accuracy. Table 3 compares the mini-batch SGD with hierarchical local SGD for fixed product $H \cdot H^b = 16$ under different network topologies, with the same training configurations. We can observe that for a heterogeneous system with a sufficient block size (e.g., the number of intra-node devices), hierarchical local SGD with sufficient number of block update steps H^b can further improve the generalization performance of local SGD training. More precisely, when $H \cdot H^b$ is fixed, hierarchical local SGD with more frequent inner-node synchronizations ($H^b > 1$) outperforms local SGD ($H^b = 1$), while still maintaining the benefits of significantly reduced communication by the inner synchronizations within each node. In summary, as witnessed by Tables 2 and 3, *hierarchical local SGD outperforms both local SGD and mini-batch SGD in terms of training speed as well as model performance*, especially for the training across nodes where inter-node connection is

Table 3. The performance of training **CIFAR-10** with **ResNet-20** via **hierarchical local SGD** on a 16-GPU Kubernetes cluster. We simulate three different types of cluster topology, namely 8 nodes with 2 GPUs/node, 4 nodes with 4 GPUs/node, and 2 nodes with 8 GPUs/node. The configuration of hierarchical local SGD satisfies $H \cdot H^b = 16$. All variants either synchronize within each node or over all GPUs, and the number of synchronization rounds is estimated by only considering $H \cdot H^b = 16$ model updates during the training (the update could come from a different level of the synchronizations). The reported results are the average of three runs and all the experiments are under the same training configurations, training for the equivalent of 300 epochs, without specific tuning.

	$H = 1, H^b = 16$	$H = 2, H^b = 8$	$H = 4, H^b = 4$	$H = 8, H^b = 2$	$H = 16, H^b = 1$
# of sync. over nodes	1	1	1	1	1
# of sync. within node	15	7	3	1	0
Test acc. on 8×2 -GPU	90.02 ± 0.28	90.25 ± 0.08	89.95 ± 0.19	91.41 ± 0.23	
Test acc. on 4×4 -GPU	91.65 ± 0.06	91.26 ± 0.17	91.46 ± 0.24	91.91 ± 0.16	91.18 ± 0.02
Test acc. on 2×8 -GPU	92.14 ± 0.10	92.05 ± 0.14	91.94 ± 0.09	91.56 ± 0.18	

slow but intra-node communication is more efficient.

5 DISCUSSION AND FUTURE WORK

Data distribution patterns. In our experiments the dataset is globally shuffled once per epoch and each local worker only accesses a disjoint part of the training data. Removing shuffling altogether, and instead keeping the disjoint data parts completely local during training might be envisioned for extremely large datasets which can not be shared, or also in a federated scenario where data locality is a must for privacy reasons. This scenario is not covered by the current theoretical understanding of local SGD, but will be interesting to investigate theoretically and practically.

Better learning rate scheduler. We have shown in our experiments that local SGD delivers consistent and significant improvements over the state-of-the-art performance of mini-batch SGD. For ImageNet, we simply applied the same configuration of “large-batch learning tricks” by (Goyal et al., 2017). However, this set of tricks was specifically developed and tuned for mini-batch SGD only, not for local SGD. For example, scaling the learning rate w.r.t. the global mini-batch size ignores the frequent local updates where each local model only accesses local mini-batches for most of the time. Therefore, it is expected that specifically deriving and tuning a learning rate scheduler for local SGD would lead to even more drastic improvements over mini-batch SGD, especially on larger tasks such as ImageNet.

Adaptive local SGD. As local SGD achieves better generalization than current mini-batch SGD approaches, an interesting question is if the number of local update steps H could be chosen adaptively, i.e. change during the training phase. This could potentially eliminate or at least simplify complex learning rate schedules. Furthermore, recent work by (Loshchilov & Hutter, 2016; Huang et al., 2017) leverages cyclic learning rate schedules either improving the anytime performance of deep neural network training, or en-

sembling multiple neural networks at no additional training cost. Adaptive local SGD could potentially achieve similar goals with reduced training cost.

Hierarchical local SGD design with cluster topology. Hierarchical local SGD provides simple but efficient training solution for devices over the complex heterogeneous system. However, its performance might be impacted by the cluster topology. For example, the topology of 8×2 -GPU in Table 3 fails to further improve the performance of local SGD by using more frequent inner node synchronization. On the contrary, sufficient large size of the GPU block could easily benefit from the block update of hierarchical local SGD, for both of communication efficiency and training quality. The design space of hierarchical local SGD for different cluster topologies should be further investigated, e.g., to investigate the two levels of model averaging frequency (within and between blocks) in terms of convergence, and the interplay of different local minima in the case of very large number of local steps.

6 CONCLUSION

In this work, we leverage the idea of local SGD to the general setting of training in distributed and heterogeneous environments. For this, we propose a hierarchical version of local SGD that can efficiently adapt to a wide range of real-world heterogenous systems. Furthermore, we empirically study local SGD on various state-of-the-art computer vision models, demonstrating significantly improved training speed and communication efficiency compared to state-of-the-art large-batch methods, both in the hierarchical local SGD as well as flat distributed training setting.

Acknowledgements. We acknowledge funding from SNSF grant 200021_175796, as well as a Google Focused Research Award.

REFERENCES

Abadi, M., Agarwal, A., Barham, P., Brevdo, E., Chen, Z., Citro, C., Corrado, G. S., Davis, A., Dean, J., Devin, M., et al. Tensorflow: Large-scale machine learning on heterogeneous distributed systems. *arXiv preprint arXiv:1603.04467*, 2016.

Aji, A. F. and Heafield, K. Sparse communication for distributed gradient descent. *arXiv preprint arXiv:1704.05021*, 2017.

Alistarh, D., Grubic, D., Li, J., Tomioka, R., and Vojnovic, M. QSGD: Communication-efficient SGD via gradient quantization and encoding. In Guyon, I., Luxburg, U. V., Bengio, S., Wallach, H., Fergus, R., Vishwanathan, S., and Garnett, R. (eds.), *NIPS - Advances in Neural Information Processing Systems 30*, pp. 1709–1720. Curran Associates, Inc., 2017.

Alistarh, D., De Sa, C., and Konstantinov, N. The convergence of stochastic gradient descent in asynchronous shared memory. *arXiv*, March 2018.

Bijral, A. S., Sarwate, A. D., and Srebro, N. On data dependence in distributed stochastic optimization. *arXiv.org*, 2016.

Bottou, L. Large-scale machine learning with stochastic gradient descent. In Lechevallier, Y. and Saporta, G. (eds.), *COMPSTAT'2010 - Proceedings of the 19th International Conference on Computational Statistics*, pp. 177–187, 2010.

Chen, J., Pan, X., Monga, R., Bengio, S., and Jozefowicz, R. Revisiting distributed synchronous SGD. *arXiv preprint arXiv:1604.00981*, 2016.

Chen, K. and Huo, Q. Scalable training of deep learning machines by incremental block training with intra-block parallel optimization and blockwise model-update filtering. In *Acoustics, Speech and Signal Processing (ICASSP), 2016 IEEE International Conference on*, pp. 5880–5884. IEEE, 2016.

Chilimbi, T. M., Suzue, Y., Apacible, J., and Kalyanaraman, K. Project adam: Building an efficient and scalable deep learning training system. In *OSDI*, volume 14, pp. 571–582, 2014.

Dean, J., Corrado, G., Monga, R., Chen, K., Devin, M., Mao, M., Senior, A., Tucker, P., Yang, K., Le, Q. V., et al. Large scale distributed deep networks. In *Advances in neural information processing systems*, pp. 1223–1231, 2012.

Deng, J., Dong, W., Socher, R., Li, L.-J., Li, K., and Fei-Fei, L. ImageNet: A large-scale hierarchical image database. In *CVPR09*, 2009.

Goyal, P., Dollár, P., Girshick, R., Noordhuis, P., Wesolowski, L., Kyrola, A., Tulloch, A., Jia, Y., and He, K. Accurate, large minibatch SGD: Training ImageNet in 1 hour. *arXiv preprint arXiv:1706.02677*, 2017.

Gropp, W., Lusk, E., and Skjellum, A. *Using MPI: portable parallel programming with the message-passing interface*, volume 1. MIT press, 1999.

He, K., Zhang, X., Ren, S., and Sun, J. Delving deep into rectifiers: Surpassing human-level performance on imagenet classification. In *Proceedings of the IEEE international conference on computer vision*, pp. 1026–1034, 2015.

He, K., Zhang, X., Ren, S., and Sun, J. Deep residual learning for image recognition. In *Proceedings of the IEEE Conference on Computer Vision and Pattern Recognition*, pp. 770–778, 2016a.

He, K., Zhang, X., Ren, S., and Sun, J. Identity mappings in deep residual networks. In *European Conference on Computer Vision*, pp. 630–645. Springer, 2016b.

Hoffer, E., Hubara, I., and Soudry, D. Train longer, generalize better: closing the generalization gap in large batch training of neural networks. *arXiv preprint arXiv:1705.08741*, 2017.

Huang, G., Liu, Z., Weinberger, K. Q., and van der Maaten, L. Densely connected convolutional networks. *arXiv preprint arXiv:1608.06993*, 2016a.

Huang, G., Sun, Y., Liu, Z., Sedra, D., and Weinberger, K. Q. Deep networks with stochastic depth. In *European Conference on Computer Vision*, pp. 646–661. Springer, 2016b.

Huang, G., Li, Y., Pleiss, G., Liu, Z., Hopcroft, J. E., and Weinberger, K. Q. Snapshot ensembles: Train 1, get m for free. *arXiv preprint arXiv:1704.00109*, 2017.

Keskar, N. S., Mudigere, D., Nocedal, J., Smelyanskiy, M., and Tang, P. T. P. On large-batch training for deep learning: Generalization gap and sharp minima. *arXiv preprint arXiv:1609.04836*, 2016.

Konecný, J., McMahan, B., and Ramage, D. Federated optimization: Distributed optimization beyond the datacenter. *arXiv preprint arXiv:1511.03575*, 2015.

Konecný, J., McMahan, H. B., Yu, F. X., Richtarik, P., Suresh, A. T., and Bacon, D. Federated learning: Strategies for improving communication efficiency. *arXiv preprint arXiv:1610.05492*, 2016.

Krizhevsky, A. and Hinton, G. Learning multiple layers of features from tiny images. 2009.

Lacoste-Julien, S., Schmidt, M., and Bach, F. A simpler approach to obtaining an $o(1/t)$ convergence rate for the projected stochastic subgradient method. *arXiv preprint arXiv:1212.2002*, 2012.

Li, M. *Scaling distributed machine learning with system and algorithm co-design*. PhD thesis, Intel, 2017.

Li, M., Zhang, T., Chen, Y., and Smola, A. J. Efficient mini-batch training for stochastic optimization. In *Proceedings of the 20th ACM SIGKDD international conference on Knowledge discovery and data mining*, pp. 661–670. ACM, 2014.

Lin, Y., Han, S., Mao, H., Wang, Y., and Dally, W. J. Deep gradient compression: Reducing the communication bandwidth for distributed training. *arXiv preprint arXiv:1712.01887*, 2017.

Loshchilov, I. and Hutter, F. SGDR: stochastic gradient descent with restarts. *arXiv preprint arXiv:1608.03983*, 2016.

McDonald, R., Mohri, M., Silberman, N., Walker, D., and Mann, G. S. Efficient large-scale distributed training of conditional maximum entropy models. In Bengio, Y., Schuurmans, D., Lafferty, J. D., Williams, C. K. I., and Culotta, A. (eds.), *Advances in Neural Information Processing Systems 22*, pp. 1231–1239. Curran Associates, Inc., 2009.

McMahan, B., Moore, E., Ramage, D., Hampson, S., and y Arcas, B. A. Communication-efficient learning of deep networks from decentralized data. In *Artificial Intelligence and Statistics*, pp. 1273–1282, 2017.

Paszke, A., Gross, S., Chintala, S., Chanan, G., Yang, E., DeVito, Z., Lin, Z., Desmaison, A., Antiga, L., and Lerer, A. Automatic differentiation in PyTorch. 2017.

Rabenseifner, R. Optimization of collective reduction operations. In *International Conference on Computational Science*, pp. 1–9. Springer, 2004.

Russakovsky, O., Deng, J., Su, H., Krause, J., Satheesh, S., Ma, S., Huang, Z., Karpathy, A., Khosla, A., Bernstein, M., et al. Imagenet large scale visual recognition challenge. *International Journal of Computer Vision*, 115(3): 211–252, 2015.

Seide, F. and Agarwal, A. CNTK: Microsoft's open-source deep-learning toolkit. In *Proceedings of the 22nd ACM SIGKDD International Conference on Knowledge Discovery and Data Mining*, pp. 2135–2135. ACM, 2016.

Shalev-Shwartz, S., Singer, Y., Srebro, N., and Cotter, A. Pegasos: Primal estimated sub-gradient solver for SVM. *Mathematical Programming*, 127(1):3–30, 2010.

Simonyan, K. and Zisserman, A. Very deep convolutional networks for large-scale image recognition. *arXiv preprint arXiv:1409.1556*, 2014.

Stich, S. U. Local SGD converges fast and communicates little. *arXiv preprint arXiv:1805.09767*, 2018.

Strom, N. Scalable distributed dnn training using commodity gpu cloud computing. In *INTERSPEECH*, pp. 1488–1492. ISCA, 2015.

Takáč, M., Bijral, A., Richtárik, P., and Srebro, N. Mini-batch primal and dual methods for SVMs. In *ICML 2013 - Proceedings of the 30th International Conference on Machine Learning*, March 2013.

Thakur, R., Rabenseifner, R., and Gropp, W. Optimization of collective communication operations in MPICH. *The International Journal of High Performance Computing Applications*, 19(1):49–66, 2005.

Wang, J., Wang, W., and Srebro, N. Memory and communication efficient distributed stochastic optimization with minibatch prox. In *ICML 2017 - Proceedings of the 34th International Conference on Machine Learning*, pp. 1882–1919. June 2017.

Wen, W., Xu, C., Yan, F., Wu, C., Wang, Y., Chen, Y., and Li, H. TernGrad: Ternary gradients to reduce communication in distributed deep learning. *arXiv preprint arXiv:1705.07878*, 2017.

You, Y., Zhang, Z., Demmel, J., Keutzer, K., and Hsieh, C.-J. ImageNet training in 24 minutes. *arXiv preprint arXiv:1709.05011*, 2017a.

You, Y., Zhang, Z., Hsieh, C.-J., and Demmel, J. 100-epoch ImageNet training with AlexNet in 24 minutes. *arXiv preprint arXiv:1709.05011*, 2017b.

Yu, H., Yang, S., and Zhu, S. Parallel restarted SGD for non-convex optimization with faster convergence and less communication. *arXiv preprint arXiv:1807.06629*, 2018.

Zagoruyko, S. and Komodakis, N. Wide residual networks. *arXiv preprint arXiv:1605.07146*, 2016.

Zhang, J., De Sa, C., Mitliagkas, I., and Ré, C. Parallel SGD: When does averaging help? *arXiv*, 2016.

Zhang, S., Choromanska, A. E., and LeCun, Y. Deep learning with elastic averaging SGD. In *NIPS 2015 - Advances in Neural Information Processing Systems 28*, pp. 685–693, 2015.

Zhou, F. and Cong, G. On the convergence properties of a k-step averaging stochastic gradient descent algorithm for

nonconvex optimization. In *Proceedings of the Twenty-Seventh International Joint Conference on Artificial Intelligence, IJCAI-18*, pp. 3219–3227. International Joint Conferences on Artificial Intelligence Organization, 7 2018. doi: 10.24963/ijcai.2018/447.

Zhou, S., Wu, Y., Ni, Z., Zhou, X., Wen, H., and Zou, Y. DoReFa-Net: Training low bitwidth convolutional neural networks with low bitwidth gradients. *arXiv preprint arXiv:1606.06160*, 2016.

Zinkevich, M., Weimer, M., Li, L., and Smola, A. J. Parallelized stochastic gradient descent. In *Advances in neural information processing systems*, pp. 2595–2603, 2010a.

Zinkevich, M. A., Weimer, M., Smola, A. J., and Li, L. Parallelized stochastic gradient descent. *NIPS 2010: Advances in Neural Information Processing Systems 23*, pp. 1–37, 2010b.

A THE ALGORITHM OF LOCAL SGD AND HIERARCHICAL LOCAL SGD

Algorithm 1 *Local SGD*

input: the initial model $\mathbf{w}_{(0)}$;
input: training data with labels \mathcal{I} ;
input: minibatch of size B_{loc} per local model;
input: step size η , and momentum m (optional);
input: number of synchronization steps T ;
input: number of local update steps H ;
input: number of nodes K .
 1: synchronize to have the same initial models $\mathbf{w}_{(0)}^k := \mathbf{w}_{(0)}$.
 2: **for all** $k := 1, \dots, K$ **do in parallel**
 3: **for** $t := 1, \dots, T$ **do**
 4: **for** $h := 1, \dots, H$ **do**
 5: sample a mini-batch from $\mathcal{I}_{(t)+h-1}^k$.
 6: compute the gradient

$$\mathbf{g}_{(t)+h-1}^k := \frac{1}{B_{\text{loc}}} \sum_{i \in \mathcal{I}_{(t)+h-1}^k} \nabla f_i(\mathbf{w}_{(t)+h-1}^k).$$

 7: update the local model to

$$\mathbf{w}_{(t)+h}^k := \mathbf{w}_{(t)+h-1}^k - \gamma_{(t)} \mathbf{g}_{(t)+h-1}^k.$$

 8: **end for**
 9: all-reduce aggregation of the gradients

$$\Delta_{(t)}^k := \mathbf{w}_{(t)}^k - \mathbf{w}_{(t)+H}^k.$$

 10: get new global (synchronized) model $\mathbf{w}_{(t+1)}^k$ for all K nodes:

$$\mathbf{w}_{(t+1)}^k := \mathbf{w}_{(t)}^k - \gamma_{(t)} \frac{1}{K} \sum_{i=1}^K \Delta_{(t)}^k$$

 11: **end for**
 12: **end for**

Algorithm 2 Hierarchical Local SGD

input: the initial model $\mathbf{w}_{[(0)]}$;
input: training data with labels \mathcal{I} ;
input: minibatch of size B_{loc} per local model;
input: step size η , and momentum m (optional);
input: number of synchronization steps T over nodes;
input: number of local update steps H ;
input: number of block update steps H^b ;
input: number of nodes K in total;
input: number of nodes K' per GPU-block.

1: synchronize to have the same initial models $\mathbf{w}_{[(0)]} := \mathbf{w}_{[(0)]}$.
 2: **for all** $k := 1, \dots, K$ **do in parallel**
 3: **for** $t := 1, \dots, T$ **do**
 4: **for** $l := 1, \dots, H^b$ **do**
 5: **for** $h := 1, \dots, H$ **do**
 6: sample a mini-batch from $\mathcal{I}_{[(t)+l]+h-1}^k$.
 7: compute the gradient

$$\mathbf{g}_{[(t)+l]+h-1}^k := \frac{1}{B_{\text{loc}}} \sum_{i \in \mathcal{I}_{[(t)+l]+h-1}^k} \nabla f_i(\mathbf{w}_{[(t)+l]+h-1}^k) .$$

8: update the local model

$$\mathbf{w}_{[(t)+l]+h}^k := \mathbf{w}_{[(t)+l]+h-1}^k - \gamma_{[(t)]} \mathbf{g}_{[(t)+l]+h-1}^k .$$

9: **end for**
 10: all-reduce aggregation of the gradients

$$\Delta_{[(t)+l]}^k := \mathbf{w}_{[(t)+l]}^k - \mathbf{w}_{[(t)+l]+H}^k .$$

11: get new block (synchronized) model $\mathbf{w}_{[(t)+l+1]}^k$ for K' block nodes:

$$\mathbf{w}_{[(t)+l+1]}^k := \mathbf{w}_{[(t)+l]}^k - \gamma_{[(t)]} \frac{1}{K'} \sum_{k=1}^{K'} \Delta_{[(t)+l]}^k ,$$

12: **end for**
 13: all-reduce aggregation of the gradients

$$\Delta_{[(t)]}^k := \mathbf{w}_{[(t)]}^k - \mathbf{w}_{[(t)+H^b]}^k .$$

14: get new global (synchronized) model $\mathbf{w}_{[(t+1)]}^k$ for all K nodes:

$$\mathbf{w}_{[(t+1)]}^k := \mathbf{w}_{[(t)]}^k - \gamma_{[(t)]} \frac{1}{K} \sum_{i=1}^K \Delta_{[(t)]}^k .$$

15: **end for**
 16: **end for**

B COMMUNICATION SCHEMES

This section evaluates the communication cost in terms of local update step and block update step, and formalizes the whole communication problem below.

Assume K computing devices uniformly distributed over K' servers, where each server has $\frac{K}{K'}$ devices. The hierarchical local SGD training procedure will access N total samples with local mini-batch size B , with H local update steps and H^b block update steps.

The MPI communication scheme (Gropp et al., 1999) is introduced for communication cost evaluation. More precisely, we use general all-reduce, e.g., *recursive halving and doubling algorithm* (Thakur et al., 2005; Rabenseifner, 2004), for gradient aggregation among K computation device. For each all-reduce communication, it introduces $C \cdot \log_2 K$ communication cost, where C is the message transmission time plus network latency.

The communication cost under our hierarchical local SGD setting is mainly determined by local step and block step. The $\frac{K}{T}$ models within each server synchronize the gradients for every H local mini-batch, and it only performs global gradients aggregation of K local models after H^b block updates. Thus, the total number of synchronizations among compute devices is reduced to $\lceil \frac{N}{KB \cdot HH^b} \rceil$, and we can formulate the overall communication cost \tilde{C} as:

$$\tilde{C} \approx \left(\lceil \frac{N}{KB \cdot H} \rceil - \lceil \frac{N}{KB \cdot HH^b} \rceil \right) \cdot C_1 \cdot K' \log_2 \frac{K}{K'} + \lceil \frac{N}{KB \cdot HH^b} \rceil \cdot C_2 \log_2 K \quad (6)$$

where C_1 is the single message passing cost for compute devices within the same server, C_2 is the cost of that across servers, and obviously $C_1 \ll C_2$. We can easily witness that the number of block step H^b is more deterministic in terms of communication reduction than local step H . Empirical evaluations can be found in Section 4.3.

Also, note that our hierarchical local SGD is orthogonal to the implementation of gradient aggregation (Goyal et al., 2017) optimized for the hardware, but focusing on overcoming the aggregation cost of a more general distributed scenarios, and can be easily integrated with any optimized all-reduce implementation.

C LARGE BATCH LEARNING TRICKS

The work of (Goyal et al., 2017) proposes common configurations to tackle large-batch training for the ImageNet dataset. We specifically refer to their crucial techniques w.r.t. learning rate as “large batch learning tricks” in our main text. For a precise definition, this is formalized by the following two configurations:

- **Scaling the learning rate:** When the global mini-batch size B_{glob} is calculated by local mini-batch size B_{loc} multiplied by K , multiply the learning rate by K .
- **Learning rate gradual warm-up:** We gradually ramp up the learning rate from a small to a large value. In (our) experiments, with a large mini-batch of size KB_{loc} , we start from a learning rate of γ and increment it by a constant amount at each iteration such that it reaches $\hat{\gamma} = K\gamma$ after 5 epochs. More precisely, the incremental step size for each iteration is calculated from $\frac{\hat{\gamma} - \gamma}{5N/(KB_{\text{loc}})}$, where N is the number of total training samples, K is the number of computing units and B_{loc} is the local mini-batch size.

D PRACTICAL IMPROVEMENTS TO LOCAL SGD TRAINING

D.1 When Local SGD meets Momentum Schemes

Momentum mini-batch SGD is widely used in place of vanilla SGD. The distributed mini-batch SGD with vanilla momentum on K training nodes follows

$$\mathbf{u}_{(t)} = m\mathbf{u}_{(t-1)} + \frac{1}{K} \sum_{k=1}^K \nabla_{(t)}^k, \quad \mathbf{w}_{(t+1)} = \mathbf{w}_{(t)} - \gamma \mathbf{u}_{(t)}$$

where $\nabla_{(t)}^k = \frac{1}{|\mathcal{I}_{(t)}^k|} \sum_{i \in \mathcal{I}_{(t)}^k} \nabla f_i(\mathbf{w}_{(t)})$.

After H updates of mini-batch SGD, we have the following updated $\mathbf{w}_{(t+H)}$:

$$\mathbf{w}_{(t+H)} = \mathbf{w}_{(t)} - \gamma \left(\sum_{\tau=1}^H m^\tau \mathbf{u}_{(\tau-1)} + \sum_{\tau=0}^{H-1} \frac{m^\tau}{K} \sum_{k=1}^K \nabla_{(t)}^k + \dots + \sum_{\tau=0}^0 \frac{m^\tau}{K} \sum_{k=1}^K \nabla_{(t+H-1)}^k \right)$$

Coming back to the setting of local SGD, it is straightforward that we can apply momentum acceleration on each local model, or on global level (Chen & Huo, 2016). In the left of this section, we analyze the case of applying local momentum and global momentum. For ease of understanding, we assume the learning rate γ is the same throughout the H update steps.

D.1.1 Local SGD with Local Momentum

When applying local momentum on the local SGD, i.e., use independent identical momentum acceleration for each local model and only globally aggregate the gradients at the time $(t) + H$, we have the following local update scheme

$$\mathbf{u}_{(t)}^k = m \mathbf{u}_{(t-1)}^k + \nabla_{(t)}^k, \quad \mathbf{w}_{(t)+1}^k = \mathbf{w}_{(t)}^k - \gamma \mathbf{u}_{(t)}^k,$$

where $\nabla_{(t)}^k = \frac{1}{|\mathcal{I}_{(t)}^k|} \sum_{i \in \mathcal{I}_{(t)}^k} \nabla f_i(\mathbf{w}_{(t)})$. Consequently, after H local update steps,

$$\mathbf{w}_{(t)+H}^k = \mathbf{w}_{(t)}^k - \gamma \left(\sum_{\tau=1}^H m^\tau \mathbf{u}_{(\tau-1)}^k + \sum_{\tau=0}^{H-1} m^\tau \nabla_{(t)}^k + \dots + \sum_{\tau=0}^0 m^\tau \nabla_{(t+H-1)}^k \right).$$

Substitute above equation to (4), we have

$$\begin{aligned} \mathbf{w}_{(t+1)} &= \mathbf{w}_{(t)} - \frac{1}{K} \sum_{k=1}^K \gamma \left(\sum_{\tau=1}^H m^\tau \mathbf{u}_{(\tau-1)}^k \sum_{\tau=0}^{H-1} m^\tau \nabla_{(t)}^k + \dots + \sum_{\tau=0}^0 m^\tau \nabla_{(t+H-1)}^k \right) \\ &= \mathbf{w}_{(t)} - \gamma \left(\sum_{\tau=1}^H \frac{m^\tau}{K} \sum_{k=1}^K \mathbf{u}_{(\tau-1)}^k + \sum_{\tau=0}^{H-1} m^\tau \left(\frac{1}{K} \sum_{k=1}^K \nabla_{(t)}^k \right) + \dots + \sum_{\tau=0}^0 \frac{m^\tau}{K} \sum_{k=1}^K \nabla_{(t+H-1)}^k \right) \end{aligned}$$

Compare the mini-batch SGD with local momentum local SGD after H update steps (H global update steps V.S. H local update steps and 1 global update step), we can witness that the main difference of these two update schemes is the difference between $\sum_{\tau=1}^H m^\tau \mathbf{u}_{(\tau-1)}$ and $\sum_{\tau=1}^H \frac{m^\tau}{K} \sum_{k=1}^K \mathbf{u}_{(t-1)}^k$, where mini-batch SGD hold a global $\mathbf{u}_{(t-1)}$ while each local model of the local SGD has their own $\mathbf{u}_{(t-1)}^k$. We will soon see the difference between the global momentum of mini-batch SGD and the local momentum of local SGD.

D.1.2 Local SGD with Global Momentum

For global momentum local SGD, i.e., a more general variant of block momentum (Chen & Huo, 2016), we would like to only apply the momentum factor to the accumulated/synchronized gradients:

$$\begin{aligned} \mathbf{u}_{(t)} &= m \mathbf{u}_{(t-1)} + \frac{1}{\gamma} \sum_{k=1}^K \frac{1}{K} (\mathbf{w}_{(t)}^k - \mathbf{w}_{(t)+H}^k) = m \mathbf{u}_{(t-1)} + \frac{1}{\gamma} \sum_{k=1}^K \frac{1}{K} \sum_{l=0}^{H-1} \gamma \nabla_{(t)+l}^k, \\ \mathbf{w}_{(t+1)} &= \mathbf{w}_{(t)} - \gamma \mathbf{u}_{(t)} = \mathbf{w}_{(t)} - \gamma \left(m \mathbf{u}_{(t-1)} + \sum_{l=0}^{H-1} \sum_{k=1}^K \frac{1}{K} \nabla_{(t)+l}^k \right) \end{aligned}$$

where $\mathbf{w}_{(t)+H}^k = \mathbf{w}_{(t)}^k - \gamma \sum_{l=0}^{H-1} \nabla_{(t)+l}^k = \mathbf{w}_{(t)}^k - \gamma \sum_{l=0}^{H-1} \nabla_{(t)+l}^k$. Note that for local SGD, we consider summing the gradients from each local update, i.e., the model difference before and after one global synchronization, and then apply the global momentum to the gradients over workers over previous local update steps.

Obviously, there exists a significant difference between mini-batch momentum SGD and global momentum local SGD, at least the term $\sum_{\tau=0}^H m^\tau$ is canceled.

D.1.3 Local SGD with Hybrid Momentum

The following equation tries to combine local momentum with global momentum, which shows how the naive implementation of local momentum and global momentum will be.

First of all, based on the local momentum scheme, after H local update steps,

$$\mathbf{w}_{(t)+H}^k = \mathbf{w}_{(t)}^k - \gamma \left(\sum_{\tau=1}^H m^\tau \mathbf{u}_{(t-1)}^k + \sum_{\tau=0}^{H-1} m^\tau \nabla_{(t)}^k + \dots + \sum_{\tau=0}^0 m^\tau \nabla_{(t)+H-1}^k \right)$$

Together the result from local momentum with the global momentum, we have

$$\begin{aligned} \mathbf{u}_{(t)} &= m\mathbf{u}_{(t-1)} + \frac{1}{\gamma} \sum_{k=1}^K \frac{1}{K} (\mathbf{w}_{(t)}^k - \mathbf{w}_{(t)+H}^k) \\ \mathbf{w}_{(t+1)} &= \mathbf{w}_{(t)} - \gamma \mathbf{u}_{(t)} \\ &= \mathbf{w}_{(t)} - \gamma \left[m\mathbf{u}_{(t-1)} + \frac{1}{\gamma} \sum_{k=1}^K \frac{1}{K} (\mathbf{w}_{(t)}^k - \mathbf{w}_{(t)+H}^k) \right] \\ &= \mathbf{w}_{(t)} - \gamma \left[m\mathbf{u}_{(t-1)} + \sum_{\tau=1}^H \frac{m^\tau}{K} \sum_{k=1}^K \mathbf{u}_{(t-1)}^k + \sum_{\tau=0}^{H-1} \frac{m^\tau}{K} \sum_{k=1}^K \nabla_{(t)}^k + \dots + \sum_{\tau=0}^0 \frac{m^\tau}{K} \sum_{k=1}^K \nabla_{(t)+H-1}^k \right] \end{aligned}$$

where $\mathbf{u}_{(t-1)}$ is the global momentum memory and $\mathbf{u}_{(t-1)}$ is the local momentum memory for each node k .

D.1.4 Local SGD with Momentum in Practice

In practice, it is suggested to combine the local momentum with global momentum to further improve the model performance.

The results reported in the main paper only apply the simple but efficient local momentum scheme. In addition to that, we slightly investigate the impact of different momentum schemes on CIFAR-10 trained with ResNet-20 on a 5×2 -GPU cluster in Table 6 and Table 7. Table 6 indicates that some factors of global momentum could further slightly improve the final test accuracy. More estimation w.r.t. different local update steps of the local SGD training can refer to Table 7.

E EXPERIMENTAL SETUP FOR CONVEX EXPERIMENTS (FIGURES 4 AND 5)

For the illustrative experiments in Section 3.4 we consider convergence of local SGD on the logistic regression problem, $f(\mathbf{w}) = \frac{1}{n} \sum_{i=1}^n \log(1 + \exp(-b_i \mathbf{a}_i^\top \mathbf{w})) + \frac{\lambda}{2} \|\mathbf{w}\|^2$, where $\mathbf{a}_i \in \mathbb{R}^d$ and $b_i \in \{-1, +1\}$ are the data samples, and regularization parameter $\lambda = 1/n$. For each run, we initialize $\mathbf{w}_0 = \mathbf{0}_d$ and measure the number of stochastic gradient evaluations (and communication rounds) until the best of last iterate and weighted average of the iterates reaches the target accuracy $f(\mathbf{w}_t) - f^* \leq \epsilon := 0.005$, with $f^* := 0.126433176216545$. For each configuration (K, H, B_{loc}) , we report the best result found with any of the following two stepsizes: $\gamma_t := \min(32, \frac{cn}{t+1})$ and $\gamma_t = 32c$. Here c is a parameter that can take the values $c = 2^i$ for $i \in \mathbb{Z}$. For each stepsize we determine the best parameter c by a grid search, and consider parameter c optimal, if parameters $\{2^{-2}c, 2^{-1}c, 2c, 2^2c\}$ yield worse results (i.e. more iterations to reach the target accuracy).

F ADDITIONAL DEEP LEARNING EXPERIMENTAL SETUP AND RESULTS

F.1 Model Selection

The scaling ratio (You et al., 2017a) identifies the ratio between computation and communication, wherein DNN models, the computation is proportional to the number of floating point operations required for processing an input while the communication is proportional to model size (or the number of parameters).

Our local SGD training scheme will show more advantages over models with small ‘‘computation and communication scaling ratio’’.

Table 4. Scaling ratio for different models.

Model	Communication # parameters	Computation # flops per image	Computation/Communication scaling ratio
ResNet-20 (CIFAR-10)	0.27 million	0.041 billion	151.85
ResNet-20 (CIFAR-100)	0.27 million	0.041 billion	151.85
ResNet-50 (ImageNet-1k)	25.00 million	7.7 billion	308.00
DenseNet-40-12 (CIFAR-10)	1.06 million	0.28 billion	264.15
DenseNet-40-12 (CIFAR-100)	1.10 million	0.28 billion	254.55
WideResNet-28-10 (CIFAR-10)	36.48 million	5.24 billion	143.64
WideResNet-28-10 (CIFAR-100)	36.54 million	5.24 billion	143.40

F.2 Local SGD Training Results

F.2.1 An Evaluation of Mini-batch SGD and Local SGD on Different Models

Table 5 demonstrates an example that we can easily train state-of-the-art compute vision models through local SGD, with significantly reduced training time.

Table 5. A complete performance demonstration of two training schemes (i.e., **mini-batch SGD** and **local SGD**) on different models for **CIFAR-10** and **CIFAR-100** (2×1 -GPU). Note that regardless of the training scheme, the model is trained from the same hyper-parameter configuration, e.g., access to the same number of samples. We can witness that local SGD could achieve similar performance as mini-batch SGD, while enjoying the benefits of less communication traffic. The performance of local SGD could be further improved while keeping the property of communication efficiency, following the configurations (Goyal et al., 2017) mentioned in Section D.

	CIFAR-10		CIFAR-100	
	Test Top-1 Accuracy	Running Time (hour)	Test Top-1 Accuracy	Running Time (hour)
ResNet-20 (K=2, H=1)	92.63 ± 0.07	2.42	68.84 ± 0.06	2.47
ResNet-20 (K=2, H=8)	92.61 ± 0.14	1.55	68.03 ± 0.04	1.55
DenseNet-40-12 (K=2, H=1)	94.41 ± 0.14	5.25	73.71 ± 0.14	5.27
DenseNet-40-12 (K=2, H=8)	94.41 ± 0.16	3.77	74.00 ± 0.12	3.78
WideResNet-28-10 (K=2, H=1)	95.89 ± 0.00	18.15	79.78 ± 0.16	19.08
WideResNet-28-10 (K=2, H=8)	95.83 ± 0.10	12.30	79.76 ± 0.02	12.78

F.2.2 Small Scale Local SGD Experiments

Figure 10 trains CIFAR-100 with ResNet-20 via local SGD on 2×1 -GPU.

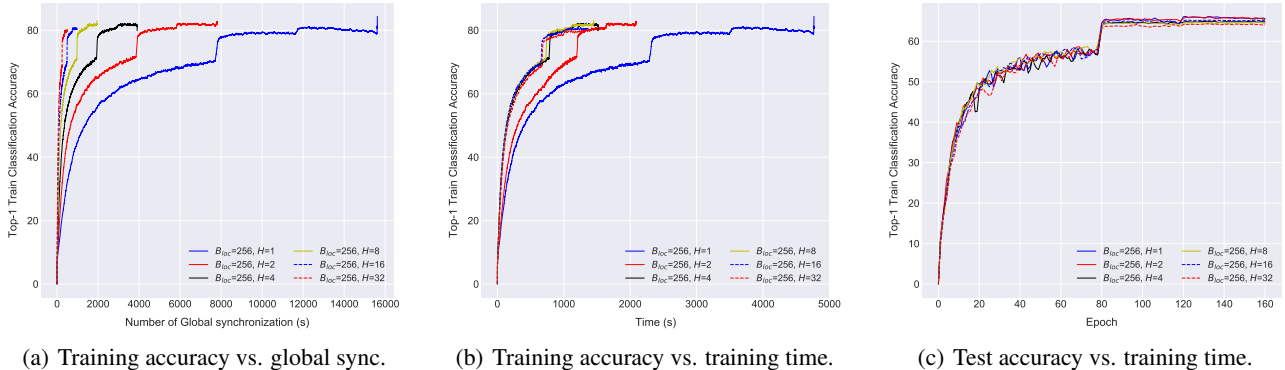


Figure 10. Train **CIFAR-100** via **Local SGD** on 2×1 -GPU. The local batch size B_{loc} is fixed to 256 for CIFAR-100, and the local step is varied from 1 to 32.

F.3 The Impact of Different Momentum Schemes

Table 6. Evaluate local momentum and global momentum for **ResNet-20** on **CIFAR-10** data via local SGD training ($H = 1$ case) on 5×2 -GPU Kubernetes cluster. The local mini-batch size is 128 and base batch size is 64 (used for learning rate linear scale). Each local model will access to a disjoint data partition, using the standard learning rate scheme as (He et al., 2016a).

local momentum	global momentum	test top-1 (10 GPUs)
0.0	0.0	90.57
0.9	0.0	92.41
0.9	0.1	92.22
0.9	0.2	92.09
0.9	0.3	92.54
0.9	0.4	92.45
0.9	0.5	92.19
0.9	0.6	91.32
0.9	0.7	18.76
0.9	0.8	14.35
0.9	0.9	12.21
0.9	0.95	10.11

Table 7. Brief performance evaluation of local momentum and global momentum on local SGD training, for **ResNet-20** with **CIFAR-10** data on 5×2 -GPU Kubernetes cluster. The local mini-batch size is 128 and base batch size is 64 (used for learning rate linear scale). Each local model will access to a disjoint data partition, using the standard learning rate scheme as (He et al., 2016a).

	$H = 8$
local momentum=0.9, global momentum=0.0	89.97
local momentum=0.9, global momentum=0.1	90.22
local momentum=0.9, global momentum=0.2	90.25
local momentum=0.9, global momentum=0.3	90.23
local momentum=0.9, global momentum=0.4	90.24
local momentum=0.9, global momentum=0.5	90.15